



ChemComm

**Synthesis and Disassembly of an Organometallic Polymer
Comprising Redox-active Co₄S₄ Clusters and Janus
Biscarbene Linkers**

Journal:	<i>ChemComm</i>
Manuscript ID	CC-COM-02-2022-000953.R1
Article Type:	Communication

SCHOLARONE™
Manuscripts

COMMUNICATION

Synthesis and Disassembly of an Organometallic Polymer Comprising Redox-active Co_4S_4 Clusters and Janus Biscarbene Linkers

Received 00th January 20xx,
Accepted 00th January 20xx

DOI: 10.1039/x0xx00000x

Jonathan H. Gillen,^a Connor A. Moore,^a My Vuong,^a Juvairia Shajahan,^b Mitchell R. Anstey,^c Jeffrey R. Alston,^b and Christopher M. Bejger^{*a}

Here, we show for the first time that main-chain organometallic polymers (MCOPs) can be prepared from Janus N-heterocyclic carbene (NHC) linkers and polynuclear cluster nodes. The crosslinked framework Co_4S_4 -MCOP is synthesized via ligand displacement reactions and undergoes reversible electron transfer in the solid state. Discrete molecular cluster species can be excised from the framework by digesting the solid in solutions of excess monocarbene. Finally, we demonstrate a synthetic route to monodisperse framework particles via coordination modulation.

Rigid, non-chelating, poly-N-heterocyclic carbene (NHC) ligands are emerging building blocks in the assembly of functional main-chain organometallic polymers (MCOPs).^{1,2} Structurally, such materials consist of bridging, poly-NHC organic linkers and single transition metal ions that serve as branching points of extension. So far, the dimensionality of this class of polymer has been dictated by the topology and geometry of the poly-NHC linker. Specifically, one,^{3,4} two,^{5–8} and three-dimensional (3D)^{9,10} MCOPs have all been reported using various poly-NHC ligands and single-metal atoms including palladium,^{3,6,9,11} platinum,¹¹ nickel,¹¹ iridium,^{4,10} and gold.^{5,7,8} Utilizing polynuclear complexes or ensembles of multiple metal atoms could afford further control over dimensionality and polymer structure. However, the investigation of NHC-based MCOPs comprising molecular clusters remains an open issue. This is surprising for several reasons. For instance, there are numerous known NHC-stabilized metal cluster compounds, including those containing metal-carbonyl¹², noble metal,^{13–15} metal-chalcogenide,^{16,17} and metal-halide¹⁸ cluster-cores. Thus, similar synthetic protocols used to prepare these discrete clusters can be applied to incorporate them into poly-NHC MCOPs. Additionally, molecular clusters are attractive from a structural standpoint. They are well-defined and can be prepared in a variety of sizes and geometries.^{19–22} In fact, the abstraction of clusters as polyhedral nodes is central to the field of reticular chemistry

and gave rise to the first crystalline metal organic frameworks (MOFs).²³ Substituting single metal atoms for clusters could, therefore, lead to crystalline NHC-MCOPs. This is significant, as all known NHC-MCOPs have all been isolated as amorphous solids. Finally, molecular cluster compounds have rich catalytic,^{24,25} photophysical,^{26,27} magnetic,^{28,29} and redox^{30–32} properties beyond what single transition metals can offer. Consequently, a diverse new class of functional MCOPs can be envisioned from the coupling of clusters with poly-NHC linkers.

Our group is using metal chalcogenide clusters as building blocks for redox active MOF-hybrids.^{33,34} This is accomplished using pre-assembled clusters stabilized with bifunctional phosphine ligands. Ancillary sites on the phosphines, and periphery of the cluster, then undergo further assembly in the presence of metal cations. However, bifunctional phosphine ligands are nonlinear linkers and produce distorted frameworks with bent connections between building units. The use of phosphine linkers thus makes the prediction of the final structure challenging, preventing the reticular design principles of MOF synthesis from being applied. Other organic ligands have been used to crosslink metal-chalcogenide clusters but suffer from similar issues. For example, coordination polymers assembled from benzenedithiolate ligands and both $[\text{Fe}_4\text{S}_4]^{2+}$ and $[\text{Mo}_3\text{S}_7]^{2+}$ clusters, respectively, have recently been reported.^{35,36} However, these polymers are 1D chains, presumably due to the flexibility and bent nature of the metal-sulfur bond between the bridging ligands and the cluster cores. Rigid, linear linkers are therefore essential in order to develop metal-chalcogenide clusters as building blocks in reticular chemistry. Here, we report that aromatic-fused, Janus di-NHC ligands are efficient bridging units for the assembly of Co_4S_4 clusters into redox active MCOPs.

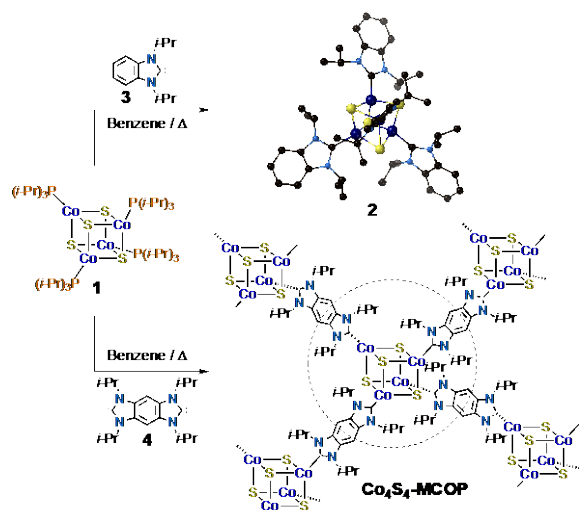
The synthetic methodology to prepare Co_4S_4 -MCOP is based on a report by Holm and coworkers that the phosphine ligated cluster $[\text{Co}_4\text{S}_4(\text{PPr}^i)_4]$ (**1**) undergoes high yielding, global ligand exchange in the presence of mono-NHC, 1,3-diisopropyl-4,5-dimethylimidazol-2-ylidene ($\text{Pr}^i_2\text{NHCMe}_2$).³⁷ This conversion can be completed in 12 hours with heating to yield the discrete cluster $\text{Co}_4\text{S}_4(\text{Pr}^i_2\text{NHCMe}_2)_4$. We prepared a benzo-bisimidazolylidene (**4**) with isopropyl “wingtips” to match the steric

^a Department of Chemistry, The University of North Carolina at Charlotte, Charlotte, NC 28223, United States.

^b The Joint School of Nanoscience and Nanoengineering, North Carolina A&T State University, Greensboro, NC 27401, United States.

^c Department of Chemistry, Davidson College, Davidson, NC 28035, United States.

*Electronic Supplementary Information (ESI) available: CCDC 2130041 and 2130042. See DOI: 10.1039/x0xx00000x



Scheme 1. Synthesis of $[\text{Co}_4\text{S}_4(\text{Pr}_2\text{NHCbz})_4]$ (**2**) and $\text{Co}_4\text{S}_4\text{-MCOP}$. Single crystal X-ray structure of **2** depicted in ball-and-stick format. Hydrogen atoms omitted.

profile of $\text{Pr}_2\text{NHCMe}_2$ using a modified prep reported by Bielawski.³⁸ The free biscarbene **4** is planar based on single-crystal X-ray diffraction (SCXRD) analysis (Fig. S1 ESI[†]). The flat, rigid nature of **4** coupled with the tetrahedral cluster core of **1** compelled us to combine the two building blocks and study their compatibility (Scheme 1). $\text{Co}_4\text{S}_4\text{-MCOP}$ is obtained as a purple solid when **1** and **4** are heated in solutions of benzene or toluene at 100 °C for 12 hours (Fig. S3 ESI[†]).

Scanning electron microscopy (SEM) and energy dispersive spectroscopy (EDS) were performed to analyze the morphology and composition of $\text{Co}_4\text{S}_4\text{-MCOP}$. SEM micrographs of the dried polymer show the material to be non-uniform in size with an irregular, foam-like morphology (Fig. S3 ESI[†]). The EDS spectra confirm the distribution of Co, S, N, and C throughout the solid (Fig. S3 ESI[†]). Trace amounts of phosphorous were also observed in some scans at the margin of the detection limit. We ascribe the presence of this intermittent phosphorous signal to residual phosphine, which could either be trapped inside the solid or still bound to a fraction of the Co_4S_4 clusters.

A zero-dimensional, molecular analog to $\text{Co}_4\text{S}_4\text{-MCOP}$ was also prepared from a comparable, benzoannulated mono-NHC ligand, Pr_2NHCbz (**3**) (Scheme 1). SCXRD analysis of $[\text{Co}_4\text{S}_4(\text{Pr}_2\text{NHCbz})_4]$ (**2**) confirmed the tetrahedral nature of the Co_4 core and the coordination of four NHC ligands around the cubane unit. This nanocluster serves as a representative fragment of $\text{Co}_4\text{S}_4\text{-MCOP}$ and was used for spectroscopic comparison to further characterize the polymeric material.

Evidence for the polymerization was first obtained via ^1H -nuclear magnetic resonance (NMR) spectroscopic studies. Specifically, when **1** and **4** were heated in C_6D_6 and monitored via NMR we observed a steady attenuation of the phosphine methine proton signal at 14.75 ppm. Concurrently, a new peak between 12 and 13.5 ppm emerged (Fig. S5 ESI[†]). This broad, new singlet matches closely to the position of the methyl protons on the discrete model cluster **2** and its appearance signifies that phosphine-NHC exchange is occurring. Full ligand substitution, however, cannot be monitored as the insoluble MCOP begins to form over time. ^{31}P -NMR spectroscopy

confirmed the formation of free phosphine under the same conditions (Fig. S7 ESI[†]). This is in accord with the biscarbene **4** effectively displacing the phosphine ligands of **1**. Unfortunately, the paramagnetic nature of both **2** and $\text{Co}_4\text{S}_4\text{-MCOP}$ precluded their analysis via solid-state ^{13}C -spectroscopy (Fig. S8 ESI[†]). Infrared (IR) spectroscopy was also performed to analyze the polymer (Fig. S9 ESI[†]). The IR spectrum of $\text{Co}_4\text{S}_4\text{-MCOP}$ contains two signals of medium intensity at 1679 and 1704 cm^{-1} , respectively. We attribute the absorbances at these frequencies to C=N stretching, due to the presence of the biscarbene linkers.³⁹ The IR spectra of cluster **2** and free biscarbene **4** also contain distinct signals in this region at 1694 and 1668 cm^{-1} , respectively. The presence of two, different C=N stretches in the polymer may be due to a mixture of free and bound **4** or sites of monotopic coordination.

X-ray photoelectron spectroscopy (XPS) measurements were collected on $\text{Co}_4\text{S}_4\text{-MCOP}$, as well as clusters **1** and **2**, to compare their elemental composition and surface valence states (Fig. S11 ESI[†]). All three samples are air sensitive and display similar oxidized cobalt and sulfur profiles upon exposure to atmosphere with characteristic peaks for the Co^{2+} oxidation state, 802.5 and 786.1 eV, and an Sp^2 peak at 161.9 eV that is indicative of a metal sulfide bond. A second sulfur peak is also observed at 166 eV, which we assign to an oxidized sulfur species (SO_x^{n-}), based on the XPS of related Co-S based solids.⁴⁰ The high-resolution XPS spectra of both $\text{Co}_4\text{S}_4\text{-MCOP}$ and **2** show the nitrogen N1s peak at approximately 400 eV. The atomic proportion of Co:S:N in cluster **2** is 5.7:4.0:9.7, while $\text{Co}_4\text{S}_4\text{-MCOP}$ has an atomic ratio of 4.6:3.8:10.7 for Co:S:N. Finally, we observed a minor quantity of phosphorous in the XPS spectrum of $\text{Co}_4\text{S}_4\text{-MCOP}$ with a low signal to noise ratio. This residual phosphorous is consonant with the trace phosphorous periodically observed during EDS measurements.

The powder X-ray diffraction (PXRD) pattern of the polymer exhibits features centered around 2.25°, 5.7°, and 13.8° 2 θ (Fig. 1a). The broad diffraction peaks are in agreement with the morphology observed via SEM and are characteristic of a disordered solid with structural defects. Observation of diffraction peaks is particularly noteworthy, as all reported NHC-MCOPs are amorphous with no measurable PXRD patterns. The small number of peaks in the experimental PXRD, however, prevent assignment of an exact structure with high certainty. Nevertheless, a theoretical unit cell of $\text{Co}_4\text{S}_4\text{-MCOP}$ assuming complete crosslinking was modeled and its PXRD pattern was simulated for comparison. The calculated pattern exhibits a number of sharp peaks clustered around 2.5° 2-theta. The center of this grouping aligns with the largest broad feature. This overlap suggests that the portions of $\text{Co}_4\text{S}_4\text{-MCOP}$ may have a 3D, diamond structure.

The electronic absorption of the polymer was studied using UV-vis spectroscopy. The UV-visible spectrum of $\text{Co}_4\text{S}_4\text{-MCOP}$ has a broad peak centered at 503 nm (Fig. 1b) and a strong absorbance below 350 nm. The optical band gap of $\text{Co}_4\text{S}_4\text{-MCOP}$ was calculated from the low energy transition to be 1.68 eV. In comparison, the spectrum of cluster **1** is less well-defined and has only one peak below 300 nm (Fig. 1b). The absorbance

profile of the polymer more resembles that of **2** dissolved in THF, with two distinct absorbance peaks (Fig. 1b).

The porosity of the polymer was analyzed using N₂ adsorption data at 77 K. Desolvated samples of Co₄S₄-MCOP exhibit a type II isotherm, with a rise in sorption at higher dinitrogen pressures (Fig. S13 ESI[†]). The Brunauer–Emmett–Teller (BET) surface area of Co₄S₄-MCOP was determined to be 22.2 m² g⁻¹. The low porosity may arise from framework collapse during solvent removal or a highly interpenetrated structure.⁴¹ Pore collapse is a common phenomenon observed when drying and removing solvents from related MOF materials.⁴² We observe a significant volume change after solvent exchange and drying. Thus, we hypothesize that a structural change followed by pore occlusion occurs under vacuum.

Thermogravimetric analysis (TGA) was performed on samples of Co₄S₄-MCOP, discrete cluster **2**, and the precursor cluster **1** to compare their thermal stabilities (Fig. 1c). All three samples undergo a similar, major weight loss below 300 °C that is likely a result of the dissociation of their organic ligands. The TGA traces reveal an increase in thermal stability as the phosphine ligands of **1** (≈ 110 °C) are substituted for NHC ligands in **2** (≈ 140 °C). Co₄S₄-MCOP is more stable than both molecular clusters **1** and **2**, exhibiting a degradation point at ≈ 240 °C. We posit that the crosslinked structure is responsible for the augmented thermal stability observed in the polymer.

Cobalt sulfide clusters are well known for their rich electrochemistry.³² The cubane-type Co₄S₄ clusters are no exception and Co₄S₄(Prⁱ₂NHCMe₂)₄ can be oxidized twice (E^{1/2} = -1.4 and E^{2/2} = -0.2 V vs. Fc/Fc⁺) to form [Co₄S₄]⁺¹ and [Co₄S₄]⁺², respectively.³⁷ Accordingly, cluster **2** also undergoes two oxidations at similar potentials (E^{1/2} = -1.7 and E^{2/2} = -0.67 V) (Fig. 1d). This prompted us to investigate the redox properties of the polymer. We prepared electrodes modified with the insoluble Co₄S₄-MCOP to study its electrochemistry in the solid state (Fig. 1d). These electrodes were submerged in solutions of MeCN with tetrabutylammonium hexafluorophosphate (TBAPF₆) supporting electrolyte and subject to cyclic voltammetry (CV) scans. The Co₄S₄-MCOP solid exhibits a single reversible redox event at -0.9 V vs Fc/Fc⁺. This potential is in a similar voltage range to the corresponding, discrete cluster **2**. Therefore, we attribute this process to the reversible oxidation of the Co₄S₄ units in the solid. The lack of other features in the CV and relative uniformity of the redox wave indicates that all cluster entities in the framework are in the equivalent oxidation state with the same supporting ligands.

Some NHC-transition metal complexes and clusters have been shown to undergo exchange with different ligand types as well as other monomeric NHCs.^{3,43,44} These reports encouraged us to mix the polymer with a monocarbene in an effort to extract a molecular species. Thus, suspensions of Co₄S₄-MCOP in C₆D₆ were heated with excess Prⁱ₂NHCMe₂ (20 equivalents). After 24 hours, a trace amount of solid remained and the solution had changed from transparent to red-brown (Fig. S16 ESI[†]). A filtered aliquot of this solution was collected and studied *via* ¹H NMR spectroscopy (Fig. 2). The spectrum of the digested sample contains diagnostic signals at 5.3 and 7.3 ppm, which

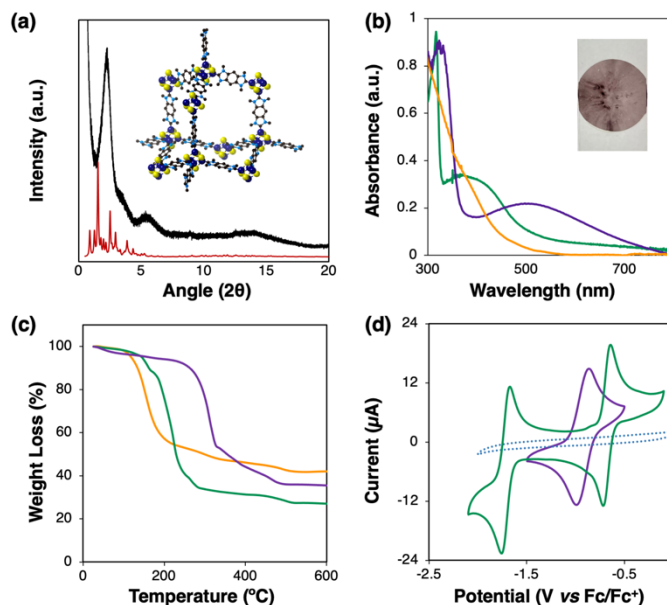


Fig. 1. (a) Synchrotron powder X-ray diffraction pattern of Co₄S₄-MCOP (black) and simulated pattern (red) of model (inset), (b) Normalized UV-vis absorption spectra (inset image of Co₄S₄-MCOP in epoxy) and (c) TGA traces of Co₄S₄-MCOP (purple), **2** (green), and **1** (orange), and (d) Cyclic voltammograms of Co₄S₄-MCOP (purple; solid-state modified glassy carbon working electrode), **2** (green), and background (blue dashed). Recorded using a GCE working electrode, Pt counter electrode, and Pt pseudo reference electrode at a scan rate of 100 mVs⁻¹ in acetonitrile with TBAPF₆ as the supporting electrolyte and referenced vs Fc/Fc⁺.

correspond to the NMR spectrum of the discrete cluster Co₄S₄(Prⁱ₂NHCMe₂)₄.³⁷ Specifically, these resonances are assigned to methyl protons on the isopropyl groups and methyl protons attached to the imidazolylidene ring, respectively. Additionally, a broad singlet was observed at -11.8 ppm. This unique resonance from the isopropyl methine protons is also consistent with the spectrum of the OD cluster and confirms that the Co₄S₄ unit can be excised from the polymer. The NMR experiment further indicates that the Co₄S₄ entity remains intact during polymerization and provides direct evidence for the dynamicity of the Co-C_{NHC} bond in the polymer.

Finally, we sought to exploit the reversible nature of the Co-C_{NHC} bonding to regulate the nucleation rate during polymerization. We hypothesized that a mono-NHC could act as a competitive capping agent (modulator) and decrease the rate of nucleation prior to solid formation. To this end, a series of solvothermal polymerizations were run in the presence of increasing equivalents of **3**. We found that larger amounts (5-15 equivalents) of modulator led to a decrease in the rate of solid formation. Polymerization does not occur at an appreciable rate under conditions of high modulator concentration (≥20 equivalents), further corroborating our observations in the digestion experiments. Precipitate isolated from reactions run in the presence of 10 equivalents of **3** also appeared markedly different via SEM (Fig. S17 ESI[†]). These modulated syntheses yielded product that was uniform in size (645 ± 166 nm), less stringy, and more particle-like than material isolated from reactions run in the absence of capping agents.

In summary, we have designed and synthesized the first example of a MCOP consisting of poly-NHC linkers and molecular cluster nodes. The material is redox active and can be depolymerized to obtain discrete, soluble Co₄S₄ entities. The rate of polymerization was found to be tunable, which may

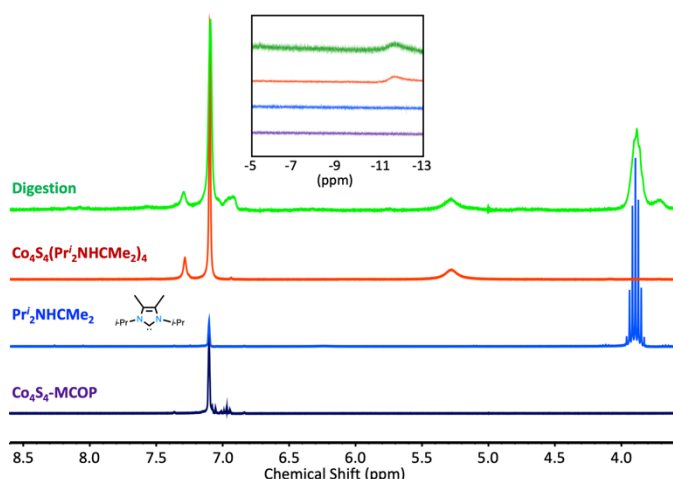


Fig 2. NMR spectra overlay of $\text{Co}_4\text{S}_4\text{-MCOP}$ before digestion (purple); $\text{Pr}_2\text{NHCMe}_2$ (blue); discrete $\text{Co}_4\text{S}_4(\text{Pr}_2\text{NHCMe}_2)_4$ (red); and mixture of $\text{Co}_4\text{S}_4\text{-MCOP}$ and $\text{Pr}_2\text{NHCMe}_2$ after digestion (green). All spectra were collected in benzene- d_6 .

provide a means to single-crystalline NHC-MCOPs in the future. Finally, this study paves the way for a new class of functional MCOPs comprising poly(NHC) ligands and clusters of different sizes, geometries, and compositions.

This work was supported by the National Science Foundation (NSF) under award number DMR-2045390. Use of the Advanced Photon Source at Argonne National Laboratory was supported by the U. S. Department of Energy, Office of Science, Office of Basic Energy Sciences, under Contract No. DE-AC02-06CH11357.

Conflicts of interest

There are no conflicts to declare.

Notes and references

- 1 Y. Wang, J.-P. Chang, R. Xu, S. Bai, D. Wang, G.-P. Yang, L.-Y. Sun, P. Li and Y.-F. Han, *Chem. Soc. Rev.*, 2021, **50**, 13559–13586.
- 2 M. Poyatos and E. Peris, *Dalt. Trans.*, 2021, **50**, 12748–12763.
- 3 A. J. Boydston, K. A. Williams and C. W. Bielawski, *J. Am. Chem. Soc.*, 2005, **127**, 12496–12497.
- 4 Z. Sun, Y. Liu, J. Chen, C. Huang and T. Tu, *ACS Catal.*, 2015, **5**, 6573–6578.
- 5 Y.-T. Wang, M.-T. Chang, G.-H. Lee, S.-M. Peng and C.-W. Chiu, *Chem. Commun.*, 2013, **49**, 7258.
- 6 C. Zhang, J.-J. Wang, Y. Liu, H. Ma, X.-L. Yang and H.-B. Xu, *Chem. - A Eur. J.*, 2013, **19**, 5004–5008.
- 7 J.-F. Longevial, M. Lo, A. Lebrun, D. Laurencin, S. Clément and S. Richeter, *Dalt. Trans.*, 2020, **49**, 7005–7014.
- 8 S. Gonell, M. Poyatos and E. Peris, *Chem. - A Eur. J.*, 2014, **20**, 5746–5751.
- 9 J. Choi, H. Y. Yang, H. J. Kim and S. U. Son, *Angew. Chemie Int. Ed.*, 2010, **49**, 7718–7722.
- 10 J. Wu, L. Shen, S. Duan, Z. N. Chen, Q. Zheng, Y. Liu, Z. Sun, J. H. Clark, X. Xu and T. Tu, *Angew. Chemie - Int. Ed.*, 2020, **59**, 13871–13878.
- 11 A. J. Boydston and C. W. Bielawski, *Dalt. Trans.*, 2006, 4073.
- 12 J. A. Cabeza and P. García-Álvarez, *Chem. Soc. Rev.*, 2011, **40**, 5389.
- 13 M. R. Narouz, K. M. Osten, P. J. Unsworth, R. W. Y. Man, K. Salorinne, S. Takano, R. Tomihara, S. Kaappa, S. Malola, C.-T. Dinh, J. D. Padmos, K. Ayoo, P. J. Garrett, M. Nambo, J. H. Horton, E. H. Sargent, H. Häkkinen, T. Tsukuda and C. M. Crudden, *Nat. Chem.*, 2019, **11**, 419–425.
- 14 M. R. Narouz, S. Takano, P. A. Lummis, T. I. Levchenko, A. Nazemi, S. Kaappa, S. Malola, G. Yousefalizadeh, L. A. Calhoun, K. G. Stamplecoskie, H. Häkkinen, T. Tsukuda and C. M. Crudden, *J. Am. Chem. Soc.*, 2019, **141**, 14997–15002.
- 15 H. Ube, Q. Zhang and M. Shionoya, *Organometallics*, 2018, **37**, 2007–2009.
- 16 L. Deng and R. H. Holm, *J. Am. Chem. Soc.*, 2008, **130**, 9878–9886.
- 17 J. L. Durham, W. B. Wilson, D. N. Huh, R. McDonald and L. F. Szczepura, *Chem. Commun.*, 2015, **51**, 10536–10538.
- 18 E. Kühnel, I. V. Shishkov, F. Rominger, T. Oeser and P. Hofmann, *Organometallics*, 2012, **31**, 8000–8011.
- 19 S. C. Lee and R. H. Holm, *Angew. Chemie Int. Ed. English*, 1990, **29**, 840–856.
- 20 R. Peng, M. Li and D. Li, *Coord. Chem. Rev.*, 2010, **254**, 1–18.
- 21 O. Fuhr, S. Dehnen and D. Fenske, *Chem. Soc. Rev.*, 2013, **42**, 1871–1906.
- 22 I. Chakraborty and T. Pradeep, *Chem. Rev.*, 2017.
- 23 M. J. Kalmutzki, N. Hanikel and O. M. Yaghi, *Sci. Adv.*, 2018, **4**.
- 24 S.-S. Wang and G.-Y. Yang, *Chem. Rev.*, 2015, **115**, 4893–4962.
- 25 M. T. Stiebritz, C. J. Hiller, N. S. Sickerman, C. C. Lee, K. Tanifuji, Y. Ohki and Y. Hu, *Nat. Catal.*, 2018, **1**, 444–451.
- 26 D. a. Morgenstern, G. M. Ferrence, J. Washington, J. I. Henderson, L. Rosenhein, J. D. Heise, P. E. Fanwick, C. P. Kubiak and W. Lafayette, *J. Am. Chem. Soc.*, 1996, **118**, 2198–2207.
- 27 T. G. Gray, C. M. Rudzinski, E. E. Meyer, R. H. Holm and D. G. Nocera, *J. Am. Chem. Soc.*, 2003, **125**, 4755–4770.
- 28 R. Winpenny, *Molecular Cluster Magnets*, WORLD SCIENTIFIC, 2011, vol. 3.
- 29 D. Maniaki, E. Pilichos and S. P. Perlepes, *Front. Chem.*, 2018, **6**, 461.
- 30 P. Baran, R. Boča, I. Chakraborty, J. Giapintzakis, R. Herchel, Q. Huang, J. E. McGrady, R. G. Raptis, Y. Sanakis and A. Simopoulos, *Inorg. Chem.*, 2008, **47**, 645–655.
- 31 C. A. Goddard, J. R. Long and R. H. Holm, *Inorg. Chem.*, 1996, **35**, 4347–4354.
- 32 P. Zanello, *Coord. Chem. Rev.*, 1988, **87**, 1–54.
- 33 A. M. Champsaur, J. Yu, X. Roy, D. W. Paley, M. L. Steigerwald, C. Nuckolls and C. M. Bejger, *ACS Cent. Sci.*, 2017, **3**, 1050–1055.
- 34 M. B. Freeman, O. D. Edokobi, J. H. Gillen, M. Kocherga, K. M. Dipple, D. S. Jones, D. W. Paley, L. Wang and C. M. Bejger, *Chem. - A Eur. J.*, 2020, **26**, 12523–12527.
- 35 N. E. Horwitz, J. Xie, A. S. Filatov, R. J. Papoular, W. E. Shepard, D. Z. Zee, M. P. Grahn, C. Gilder and J. S. Anderson, *J. Am. Chem. Soc.*, 2019, **141**, 3940–3951.
- 36 Z. Ji, C. Trickett, X. Pei and O. M. Yaghi, *J. Am. Chem. Soc.*, 2018, **140**, 13618–13622.
- 37 L. Deng, E. Bill, K. Wieghardt and R. H. Holm, *J. Am. Chem. Soc.*, 2009, **131**, 11213–11221.
- 38 J. W. Kamplain and C. W. Bielawski, *Chem. Commun.*, 2006, 1727.
- 39 Y. Wang and R. A. Poirier, *J. Phys. Chem. A*, 1997, **101**, 907–912.
- 40 X. Ma, W. Zhang, Y. Deng, C. Zhong, W. Hu and X. Han, *Nanoscale*, 2018, **10**, 4816–4824.
- 41 Y.-N. Gong, D.-C. Zhong and T.-B. Lu, *CrystEngComm*, 2016, **18**, 2596–2606.
- 42 R. A. Dodson, A. G. Wong-Foy and A. J. Matzger, *Chem. Mater.*, 2018, **30**, 6559–6565.
- 43 L. R. Titcomb, S. Caddick, F. G. N. Cloke, D. J. Wilson and D. McKerrecher, *Chem. Commun.*, 2001, 1388–1389.
- 44 S. R. Smock, R. Alimento, S. Mallikarjun Sharada and R. L. Brutchey, *Inorg. Chem.*, 2021, **60**, 13699–13706.